microPublication BIOLOGY

11/9/2026 - *Open Access*

# Comparative assessment of Dendra2 and mKikGR for *in vivo* analysis of protein turnover in *Caenorhabditis elegans*

Joren M Woeltjes[1], Loes B Steller[1], Suzan Ruijtenberg[1], Mike Boxem[1§]

[1]1. Institute of Biodynamics and Biocomplexity, Department of Biology, Utrecht University, Utrecht, UT, The Netherlands

[§]To whom correspondence should be addressed: m.boxem@uu.nl

## Abstract

Photoconvertible fluorescent proteins are used as a tool to study protein dynamics *in vivo*. Here, we directly compared the photoconvertible fluorophores Dendra2 and mKikGR in *Caenorhabditis elegans*. We endogenously tagged the brush border protein NRFL-1 and evaluated photoconversion rate, photostability, and brightness. We found that mKikGR has a higher photoconversion rate, while Dendra2 is brighter. Under common imaging conditions, there is no clear difference in photostability. Thus, for most applications, both mKikGR and Dendra2 are suitable, but Dendra2 may be advantageous for low-abundance proteins. We also show that mKikGR can be used for long-term analysis of NRFL-1 protein turnover.

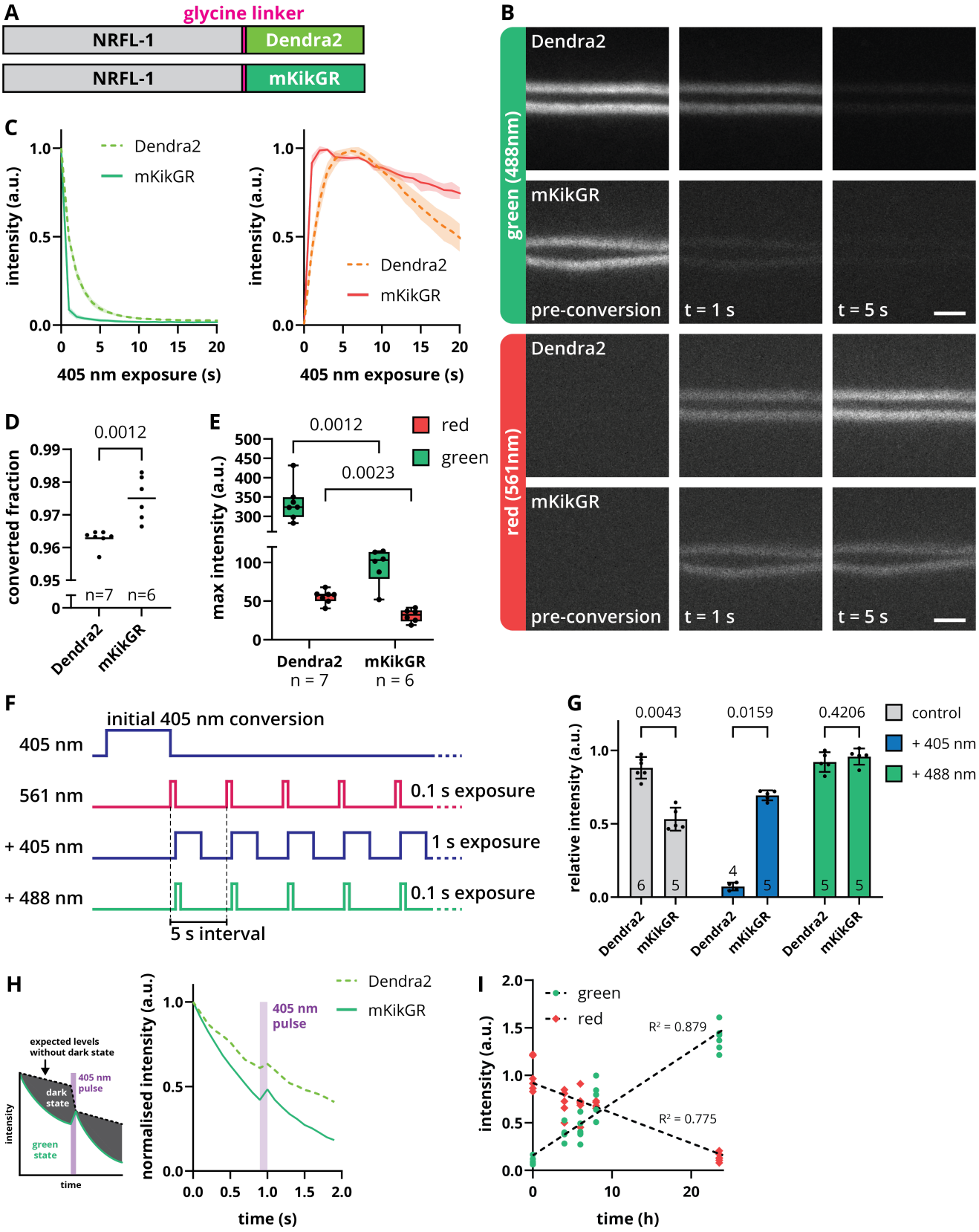



**Figure 1. Comparative assessment of Dendra2 and mKikGR:**

(A) Schematic of C-terminal Dendra2 and mKikGR fusions to NRFL-1. (B) Representative images showing NRFL-1::Dendra2 and NRFL-1::mKikGR before (left) and after photoconversion. Animals were imaged prior to conversion, and every subsequent second. In between imaging, they were exposed to a 1 second pulse of 405 nm laser light to photoconvert Dendra2 or mKikGR from green to red. (C) Average fluorescence intensity levels plotted over time. N = 5 for each condition. Lines and shaded areas plot mean ± SD. Scale bars: 2 µm. (D) Green-to-red converted fraction of

Dendra2 and mKikGR. The converted fraction was determined as the average loss of green signal over a 10 second time window after the maximum red emission time point. Each dot represents a single animal, and line the mean. Mann-Whitney test: P = 0.0012. (E) Maximum green- and red-state fluorescence intensities for Dendra2 and mKikGR. Boxes show the median and interquartile range; whiskers extend from the minimum to the maximum. Each dot represents a single animal. Mann-Whitney test; green: P = 0.0012; red: P = 0.0023. (F) Graphical representation of the experimental set-up in G. (G) Relative red-state intensity after a total of 3 seconds of 561 nm light exposure (0.1 second pulses at 5 second intervals), interspersed with either 1 second pulses of 405 nm light or 100 ms pulses of 488 nm light. Bars plot the mean ± SD. Each dot represents a single animal. Mann-Whitney test: control: P = 0.0043; +405 nm pulses: P = 0.0159; +488 nm pulses: P = 0.4206. *n* is indicated in each bar. (H) Graphical representation of expected green state levels and dark state conversion, and measured green state levels during 2 second acquisition with a single 100 ms 405 nm pulse after 1 s. n = 1 (I) Total protein turnover of NRFL-1 measured up to 24 h. Green intensity was normalized to mean pre-conversion levels, and red intensity to the mean at the first timepoint. Dotted lines are simple linear regression fits. Each dot represents a single animal. *n* = 6, 6, 6, 5, 6 for the subsequent timepoints. Different animals were imaged at each timepoint.

## Description

Photoconvertible fluorophores are a valuable tool for studying dynamic cellular processes, such as protein turnover and mobility, and for tracking cell lineages (Nemet et al., 2015). Unlike conventional fluorophores such as GFP, photoconvertible fluorophores can be irreversibly converted from one colour state to another upon illumination with a specific wavelength (Wiedenmann et al., 2004; Lešková et al., 2019). Multiple photoconvertible fluorophores have been developed over the past decades, including EosFP, Dendra, Kaede, and KikGR (Wiedenmann et al., 2004; Tsutsui et al., 2005; Gurskaya et al., 2006; Habuchi et al., 2008). As photoconvertible fluorophores can vary in conversion rate, convertible fraction, photostability, and brightness, comparing different variants can help us identify the most suitable fluorophore for a given application.

In the nematode *Caenorhabditis elegans*, Dendra2 and mKikGR have been used successfully (Hamer et al., 2010; So et al., 2024). Both are green-to-red photoconvertible fluorophores that convert upon illumination with UV (100-400 nm) or violet light (405 nm) (Tsutsui et al., 2005; Gurskaya et al., 2006; Habuchi et al., 2008). Previous data indicate that mKikGR has a high photoconversion rate and improved photostability over other photoconvertible proteins, which helps to reduce negative effects from phototoxicity (Habuchi et al., 2008; Turkowyd et al., 2017). However, in *C. elegans* a direct comparison between the mKikGR and Dendra2 photoconvertible fluorophores is lacking. Here, we aimed to directly compare the properties of these two fluorophores *in vivo* to determine their suitability for measuring protein turnover.

To determine the *in vivo* behaviour of Dendra2 and mKikGR in *C. elegans*, we generated endogenous CRISPR/Cas9-mediated fusions to NRFL-1, an abundant apical adapter protein that links the Ezrin/Radixin/Moesin ortholog ERM-1 to various other proteins (Figure 1A, Sepers et al., 2022). High expression levels and low turnover rates make NRFL-1 an ideal candidate to measure and compare photoconversion rates, convertible fraction, photostability, and brightness.

We first compared the kinetics of green-to-red photoconversion by exposing L2 larvae to repeated 1 second pulses of a 405 nm laser, interspersed with imaging of green and red fluorescence for 100 ms each. mKikGR converted from green to red faster than Dendra2 (Figure 1B, C). After two 1 second pulses of 405 nm laser exposure, green mKikGR levels decreased to less than 5% of initial levels, whereas Dendra2 required at least 8 consecutive 1 second pulses of 405 nm laser exposure to reach a comparable reduction (Figure 1B, C). The maximum fraction converted was significantly higher for mKikGR (96.3% for Dendra2 vs. 97.5% for mKikGR, P = 0.0012), although the absolute difference was modest (Figure 1D).

Next, we compared the fluorescence intensity of NRFL-1 tagged with Dendra2 or mKikGR. We measured a higher fluorescence intensity for Dendra2, particularly in the green state, where its signal was approximately 3.5-fold higher than that of mKikGR (Figure 1E). This higher brightness may make Dendra2 advantageous for visualising low-abundance proteins. However, we cannot exclude the possibility that the two fusion proteins are expressed at different levels.

To test the photostability of Dendra2 and mKikGR, we performed an initial photoconversion (2 and 5 seconds of 405 nm light for NRFL-1::mKikGR and NRFL-1::Dendra2 respectively) followed by imaging of the red fluorescent channel at 5 second intervals (561 nm, 100 ms exposures). Additionally, we tested the effect of exposing animals to either 100 ms pulses of 488 nm (blue) light (mimicking imaging of a green fluorophore) or 1 second pulses of 405 nm light in between the image acquisition (Figure 1F). In all conditions, we measured remaining red fluorescence intensity after 3 seconds total exposure time to 561 nm (green) light.

With post-conversion exposure to 561 nm light only, 88% of the red Dendra2 signal remained after 3 second total exposure, compared with only 53% for mKikGR. Interestingly, the additional exposures to 405 nm or 488 nm strongly affected the results. Exposure to 405 nm light caused a decrease in average red Dendra2 intensity from 0.88 to 0.07 a.u. (Figure 1G). Thus, Dendra2 photostability is dependent on the illumination wavelength, and reduced by exposure to 405

nm light. mKikGR was much less affected by exposure to 405 nm light. Surprisingly, however, mKikGR was more photostable when exposed to 488 nm pulses in addition to the 561 nm pulses (Figure 1G). One possibility is that red mKikGR enters a dark state upon exposure to 561 nm light, which is reversed by exposure to 488 nm light. This hypothesis is based on the observation that red EosFP switches to a dark state upon 561 nm light illumination, which can be reversed with either 405 or 488 nm light exposure (Nienhaus & Nienhaus, 2021; Wulffelé et al., 2025).

The presence of dark states may also explain a second observation we made during our analyses. We found that illumination with a 488 nm laser to focus the microscope resulted in a rapid decline in green signal intensity for both Dendra2 and mKikGR. This decrease might be attributable to conversion to reversible dark green states as opposed to bleaching, based on in-depth analyses of conformational states in the mechanistically related EosFP family and Dendra2 (De Zitter et al., 2019; De Zitter et al., 2020; Tao et al., 2020; Nienhaus & Nienhaus, 2021; Wulffelé et al., 2025). To test this, we exposed NRFL-1::Dendra2 and NRFL-1::mKikGR animals to a brief (100 ms) pulse of 405 nm light following an initial period of exposure to 488 nm light. If the loss of green intensity were due to bleaching, the 405 nm pulse would be expected to further decrease green signal due to green-to-red conversion. If, however, the loss of green intensity were due to conversion to a dark state, the 405 nm pulse would be expected to shift a portion of the protein back to the green state, in addition to the green-to-red conversion, potentially resulting in a net increase in green signal. We observed a partial recovery of green signal, consistent with the hypothesis that the decrease in green signal upon 488 nm light exposure is due to conversion to a dark conformational state (Figure 1H).

Finally, we examined whether mKikGR can be used for long-term tracking of NRFL-1 protein turnover in the intestine. We exposed L2 larvae to the 405 nm LED light source of a fluorescent binocular microscope for 10 seconds and imaged at specific timepoints thereafter. Red fluorescence corresponds to the pool of NRFL-1 present at photoconversion, whereas green fluorescence indicates newly synthesised protein. Red signal decreased by ~85% after 24 h, suggesting that protein turnover of NRFL-1 takes around 24 hours (Figure 1I). This observation is consistent with the slow turnover rate of NRFL-1 at the apical domain previously measured by fluorescence recovery after photobleaching (FRAP) (Sepers et al., 2022) and demonstrates that mKikGR is suitable for the long-term tracking of protein turnover.

In summary, we compared the *in vivo* properties of Dendra2 and mKikGR in *C. elegans* using endogenous NRFL-1 fusions, and showed that mKikGR enables tracking of protein turnover over long periods of time. mKikGR has a higher photoconversion rate than Dendra2, but is less bright, particularly in the green state. Under imaging conditions combining a brief 405 nm exposure for photoconversion with subsequent red and green state imaging, we observed no difference in photobleaching between Dendra2 and mKikGR. Finally, we observed behaviour consistent with reversible dark green conformational states for mKikGR and Dendra2 under 488 nm illumination. This effect was stronger for mKikGR, making it more difficult to use when green fluorescence is essential to focus on the sample, or where obtaining pre-conversion images is essential. Ultimately, neither fluorophore consistently outperformed the other, and both are suitable for photoconversion studies in *C. elegans*.

## Methods

### *C. elegans* maintenance

*C. elegans* strains were cultured and maintained under standard conditions (Brenner, 1974). The animals were grown on nematode growth medium (NGM) plates seeded with the *Escherichia coli* strain OP50. All experiments were performed at 20 °C.

### CRISPR/Cas9 genome editing

*C. elegans* codon-optimised Dendra2 and mKikGR were designed with the use of Wormbuilder (https://wormbuilder.org/transgenebuilder/) (Frøkjær-Jensen et al., 2016), and ordered as gBlock Gene Fragments through IDT. gBlocks were cloned into pBSK by blunt ligation to yield plasmids pSRG103 and pSRG104. A 4x Gly linker was placed between the fluorescent protein and NRFL-1. Silent mutations were introduced to prevent re-cutting after homologous recombination. The knock-in alleles were made using CRISPR/Cas9-mediated homology-directed repair in a wild-type animal (CGC1). The genomic *nrfl-1* sequence was obtained from WormBase (Sternberg et al., 2024). Young adult animals were injected with the repair template for either Dendra2 or mKikGR and the Cas9 (Alt-R S.p. Cas9 Nuclease V3)-guide RNA complex (Ghanta et al., 2021). Progeny were selected by fluorescence, and the knock-in sequences were PCR amplified and sequenced, using Sanger sequencing.

### Microscopy

The animals were handled in daylight settings, as this did not produce any measurable level of conversion. Animals were mounted on a 5% agarose pad and immobilised with 20 mM tetramisole solution in M9 (22 mM $KH_2PO_4$, 42 mM $Na_2HPO_4$, 85 mM NaCl, 1 mM $MgSO_4$). Spinning disc confocal imaging was performed on a Nikon Ti-U microscope, equipped with a Yokogawa CSU-X1 spinning disc and a Prime BSI Express Scientific CMOS camera (Teledyne Photometrics). We used a Nikon CFI Plan Apo λ 100x/1.45 0.13mm WD OIL objective for the Dendra2 and mKikGR comparisons, and a Nikon CFI Plan Apo λ 60x/1.40 0.13mm WD OIL objective for the 24 h protein turnover analysis.

Prior to imaging, the objective was manually focused on the middle of the intestine using only backlight, without the use of the lasers. Identical settings were used for both green and red channels.

**Photoconversion**

Green-to-red conversion for the Dendra2 and mKikGR comparisons was done on the Nikon spinning disc confocal microscope, using the 405 nm BFP laser at a measured power of 0.605 mW. For the 24 h protein turnover experiment, animals were converted on an Axio Zoom.V16 using blue 405 nm light for 10 seconds to ensure optimal green-to-red conversion at a measured power of 86.0 mW.

**Image analysis**

Image analysis was conducted in FIJI. A 5 pixel-wide line was drawn along sections of the brush border of the int2-4 cells, and the average intensity was measured. All images were corrected for background fluorescence by measuring an area outside of the animal and subtracting this value from the absolute measured fluorescence value.

**Statistics**

All statistical analyses were performed using GraphPad Prism (10.4.1). The sample sizes, statistical test used, and p values are indicated in the Figure and legend. No statistical method was used to pre-determine sample sizes. No samples or animals were excluded from analysis. The experiments were not randomised, and the investigators were not blinded to allocation during experiments and outcome assessment. All presented graphs were made using GraphPad Prism and Adobe Illustrator. All tests were two-tailed. All data were treated as non-normally distributed, and a Mann-Whitney test was used for all comparisons.

**Data availability**

All data supporting the findings of this study are available within the paper. Raw microscopy image files are available from the corresponding author upon reasonable request. *C. elegans* strains are available upon reasonable request.

## Reagents

| Strain | Genotype | Source |
|---|---|---|
| CGC1 | wild type | CGC |
| BOX1335 | *nrfl-1(mib377[nrfl-1::Dendra2])* IV | this study |
| BOX1336 | *nrfl-1(mib378[nrfl-1::mKikGR])* IV | this study |
| **Plasmid** | **Genotype** | **Description** |
| pSRG103 | pBSK::Dendra2 | |
| pSRG104 | pBSK::mKikGR | |
| **Oligo** | **Sequence (5'-3')** | **Description** |
| *nrfl-1* crRNA | CCTTAACGAGAAGTATCAAT | crRNA targeting *nrfl-1*; used for both knock-ins |
| Forward RT *nrfl-1::Dendra2* | ttgtagGCACGAGATGAGCCTTAACGAGAAGTATCAAT TaGTaAGtAAtATGGGCGGTGGGGGAATGAACACTCCGGG GATCAATCTG | Forward primer for amplifying the *nrfl-1::Dendra2* repair template (RT) |
| Reverse RT *nrfl-1::Dendra2* | aatagaagaaaataagaagaagttgcaaaagaTTACCA GACTTGGGATGGGAGTG | Reverse primer for amplifying the *nrfl-1::Dendra2* repair template (RT) |

| | | |
|---|---|---|
| Forward RT *nrfl-1::mKikGR* | ttgtagGCACGAGATGAGCCTTAACGAGAAGTATCAAT TaGTaAGtAatATGGGCGGTGGGGGAATGTCGGTGATCAC TTCGGAAATG | Forward primer for amplifying the *nrfl-1::mKikGR* repair template (RT) |
| Reverse RT *nrfl-1::mKikGR* | AatagaagaaaataagaagaagttgcaaaagaTTATGC CTCGAATTCGTACTTAGCTCC | Reverse primer for amplifying the *nrfl-1::mKikGR* repair template (RT) |
| Forward (genotyping) | CCATTGAGCAATGGTTCCAGC | PCR amplification and Sanger sequencing of knock-in alleles; used for both knock-ins |
| Reverse (genotyping) | cggtgtaagtaaagaatattgcacaacc | PCR amplification and Sanger sequencing of knock-in alleles; used for both knock-ins |

**Acknowledgements:** We thank W. Arkes for help with experiments. We also thank the Ruijtenberg and the Boxem lab members for their helpful discussions. This work utilised resources from Utrecht University. We also thank the Biology Imaging Center, Faculty of Sciences, of the Department of Biology at Utrecht University. Some strains were provided by the CGC, which is funded by NIH Office of Research Infrastructure Programs (P40 OD010440).

## References

Brenner S. 1974. The genetics of Caenorhabditis elegans. Genetics. 77: 71-94. 4052. DOI: 10.1093/genetics/77.1.71

De Zitter E, Thedie D, Monkemoller V, Hugelier S, Beaudouin J, Adam V, et al., Bourgeois D. 2019. Mechanistic investigation of mEos4b reveals a strategy to reduce track. Nature Methods. 16: 707-710. 4020. DOI: 10.1038/s41592-019-0462-3

De Zitter E, Ridard J, Thedie D, Adam V, Levy B, Byrdin M, et al., Bourgeois D. 2020. Mechanistic Investigations of Green mEos4b Reveal a Dynamic Long-Lived. Journal of the American Chemical Society. 142: 10978-10988. 4022. DOI: 10.1021/jacs.0c01880

Frokjaer Jensen C, Jain N, Hansen L, Davis MW, Li Y, Zhao D, et al., Fire AZ. 2016. An Abundant Class of Non-coding DNA Can Prevent Stochastic Gene Silenc. Cell. 166: 343-357. 4024. DOI: 10.1016/j.cell.2016.05.072

Ghanta KS, Ishidate T, Mello CC. 2021. Microinjection for precision genome editing in Caenorhabditis elegans. STAR protocols. 2: 100748. 4026. DOI: 10.1016/j.xpro.2021.100748

Gurskaya NG, Verkhusha VV, Shcheglov AS, Staroverov DB, Chepurnykh TV, Fradkov AF, Lukyanov S, Lukyanov KA. 2006. Engineering of a monomeric green-to-red photoactivatable fluorescent p. Nature Biotechnology. 24: 461-465. 4028. DOI: 10.1038/nbt1191

Habuchi S, Tsutsui H, Kochaniak AB, Miyawaki A, Oijen AM. 2008. mKikGR, a monomeric photoswitchable fluorescent protein. PloS One. 3: e3944. 4030. DOI: 10.1371/journal.pone.0003944

Hamer G, Matilainen O, Holmberg CI. 2010. A photoconvertible reporter of the ubiquitin-proteasome system in vivo. Nature Methods. 7: 473-478. 4032. DOI: 10.1038/nmeth.1460

Leskova A, Kusa Z, Labajova M, Krausko M, Jasik J. 2019. The Photoconvertible Fluorescent Protein Dendra2 Tag as a Tool to Inve. Methods in Molecular Biology. 1992: 201-214. 4034. DOI: 10.1007/978-1-4939-9469-4_13

Nemet I, Ropelewski P, Imanishi Y. 2015. Applications of phototransformable fluorescent proteins for tracking t. Photochemical & Photobiological Sciences: Official Journal of the Euro. 14: 1787-1806. 4036. DOI: 10.1039/c5pp00174a

Nienhaus K, Nienhaus GU. 2021. Fluorescent proteins of the EosFP clade: intriguing marker tools with. RSC chemical biology. 2: 796-814. 4038. DOI: 10.1039/d1cb00014d

Sepers JJ, Ramalho JJ, Kroll JR, Schmidt R, Boxem M. 2022. ERM-1 Phosphorylation and NRFL-1 Redundantly Control Lumen Formation i. Frontiers in Cell and Developmental Biology. 10: 769862. 1352. DOI: 10.3389/fcell.2022.769862

So S, Asakawa M, Sawa H. 2024. Distinct functions of three Wnt proteins control mirror-symmetric orga. eLife. 13: e103035. 4040. DOI: 10.7554/eLife.103035

Sternberg PW, Van Auken K, Wang Q, Wright A, Yook K, Zarowiecki M, et al., Stein L. 2024. WormBase 2024: status and transitioning to Alliance infrastructure. Genetics. 227: iyae050. 3606. DOI: 10.1093/genetics/iyae050

Tao A, Zhang R, Yuan J. 2020. Characterization of Photophysical Properties of Photoactivatable Fluor. The Journal of Physical Chemistry. B. 124: 1892-1897. 4042. DOI: 10.1021/acs.jpcb.9b11028

Tsutsui H, Karasawa S, Shimizu H, Nukina N, Miyawaki A. 2005. Semi-rational engineering of a coral fluorescent protein into an effic. EMBO reports. 6: 233-238. 4044. DOI: 10.1038/sj.embor.7400361

Turkowyd B, Balinovic A, Virant D, Carnero HGG, Caldana F, Endesfelder M, Bourgeois D, Endesfelder U. 2017. A General Mechanism of Photoconversion of Green-to-Red Fluorescent Pro. Angewandte Chemie. 56: 11634-11639. 4046. DOI: 10.1002/anie.201702870

Wiedenmann J, Ivanchenko S, Oswald F, Schmitt F, Rocker C, Salih A, Spindler KD, Nienhaus GU. 2004. EosFP, a fluorescent marker protein with UV-inducible green-to-red flu. Proceedings of the National Academy of Sciences of the United States o. 101: 15905-15910. 4048. DOI: 10.1073/pnas.0403668101

Wulffele J, Maity A, Ayala I, Gambarelli S, Brutscher B, Bourgeois D. 2025. Light-Induced Conformational Heterogeneity Induces Positive Photoswitc. Journal of the American Chemical Society. 147: 10357-10368. 4050. DOI: 10.1021/jacs.4c17311

**Funding:** Funding for this project was provided by the ERC Starting Grant 101219284 to S. Ruijtenberg

**Conflicts of Interest:** The authors declare that there are no conflicts of interest present.

**Author Contributions:** Joren M Woeltjes: conceptualization, formal analysis, investigation, writing - original draft, writing - review editing. Loes B Steller: conceptualization, investigation, writing - original draft, writing - review editing. Suzan Ruijtenberg: funding acquisition, conceptualization, supervision, writing - original draft, writing - review editing. Mike Boxem: supervision, writing - original draft, writing - review editing, conceptualization.

**Reviewed By:** Anonymous

**Nomenclature Validated By:** Anonymous

**WormBase Paper ID:** WBPaper00070263

**History: Received** September 17, 2026 **Revision Received** October 7, 2026 **Accepted** November 3, 2026 **Published Online** November 9, 2026 **Indexed** November 23, 2026

**Copyright:** © 2026 by the authors. This is an open-access article distributed under the terms of the Creative Commons Attribution 4.0 International (CC BY 4.0) License, which permits unrestricted use, distribution, and reproduction in any medium, provided the original author and source are credited.

**Citation:** Woeltjes JM, Steller LB, Ruijtenberg S, Boxem M. 2026. Comparative assessment of Dendra2 and mKikGR for *in vivo* analysis of protein turnover in *Caenorhabditis elegans*. microPublication Biology. 10.17912/micropub.biology.002425